K O N I N K L I J K N E D E R L A N D S
M E T E O R O L O G I S C H I N S T I T U U T

Wetenschappelijk Rapport W.R. 61-3

Dr. H.M. de Jong

On the possibility of improving aerological observations by using synchronous radiosonde and radar data and on a new aerological diagram

De Bilt - 1961

KONINKLIJK NEDERLANDS
METEOROLOGISCH INSTITUUT

Wetenschappelijk Rapport
W.R. 61-3
U.D.C.: 551.501.5
551.501.74
551.501.8
551.508.82a
551.547.1

Dr. H.M. de Jong

On the possibility of improving aerological observations by using synchronous radiosonde and radar data and on a new aerological diagram

CONTENTS

1. Introduction

When at an aerological station a radar instrument is available, the combination of a radiosounding and radar observation yields an overdetermined system of aerological data. In particular the height of the sounding balloon may be obtained in two different ways. It may be computed from radiosonde data only, viz. temperature, pressure and humidity or it may be determined by means of radar data, i.e. slant range and elevation angle. The "sounding height" is obtained by integrating the hydrostatic equation, the "radar height" by using goniometry.

Recently radar sets have been designed especially for balloon tracking purposes to measure wind and height data more accurately up to high levels. Some of them are tracking automatically (e.g. Selenia RMN/1C and Omera 481). Others are being operated manually (Decca W.F.1 and W.F.2). With respect to the measurement of elevation and azimuth angle these radar sets guarantee a precision comparable with that of optical theodolites, viz. better than 0,1°. With regard to the slant range, one claims an accuracy better than 100 m.

The considerable improvement in observation techniques offers the possibility to make comparative studies of sounding- and radar heights. One such investigation has been performed in De Bilt, using observations of Kew Mark II B radiosondes and the Decca windfinding radarset (Decca W.F.1). The investigation revealed that it must be worth while to eliminate observed pressure data from computations and to replace them by the radar height. In other words, when p denotes pressure, z height, Φ geopotential, T temperature and U humidity, the (P, T, U) method is to be replaced by the (z, T, U)- or the (Φ, T, U) method.

2. Comparison of the balloon height, determined by radar, respectively by radiosonde ascents

The "radar height" z in geometric units is obtained by goniometry from slant range ρ and elevation angle ε. It includes a term for the effect of the earth's curvature and it is expressed in geopotential units:

$$z = \rho \sin \varepsilon + \frac{\rho^2 \cos^2 \varepsilon}{2R} \ldots , \qquad (1)$$

where R denotes the earth's radius.

The geopotential Φ is a function of z:

$$\Phi = \Phi(z) = \frac{g_\Phi}{9.8} \frac{Rz}{R + z}$$

g_Φ is the actual acceleration of gravity at mean sea level at the given latitude. The conversion table $\Phi(z)$ can be made for the appropriate station by application of the rules in Smithsonian Tables, Ed. VI, 49-51. Thus, the "radar height" in units of geopotential, $\Phi_r(z)$, can easily be computed.

In some modern radar designs the polar coordinates: elevation angle, azimuth angle and slant range are transformed by an electronic computer into cylinder coordinates: height, distance and azimuth. Sometimes the earth's curvature effect is already included in the machine calculations.

The "sounding height" Φ_s can be derived from radiosonde data by using the hydrostatic equation and the equation of state.

In the (p, T, U) system we have

$$\Phi_s = -\int_{p_o}^{p} R\, T_v\, d \ln p \ldots \qquad (2)$$

R is the gas constant for dry air, T_v the virtual temperature. Φ_s is also expressed in geopotential units. Usually Φ_s is determined graphically in thermodynamic diagrams in which (T, p) and (U, p) graphs are plotted.

In practice both Φ_r and Φ_s are known as a function of time:

$$\Phi_r = \Phi_r(t)$$

$$\Phi_s = \Phi_s(t)$$

Φ_r and Φ_s can be represented in a (Φ, t) diagram, as is indicated in fig. 1.

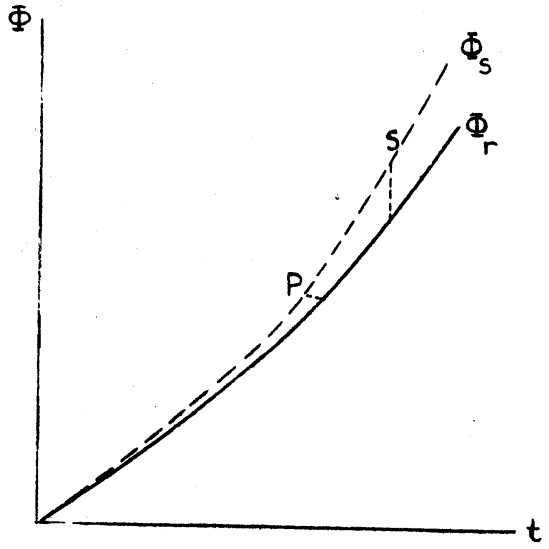

Fig. 1

The (Φ_r, t) curve is based on observations every minute, the (Φ_s, t) curve on the geopotential and time of significant points in the temperature recording.

Obviously the radar height Φ_r should at any moment be equal to the sounding height Φ_s, but an investigation of numerous radiosonde ascents has shown that considerable deviations occur.

For 18 Kew Mark II B sondes the deviations are given in table I. The deviations are assembled in classes. The number of occurrence within specified intervals for $|\Phi_r - \Phi_s|$ is noted as a function of time respectively mean balloon height. The mean balloon height is read from a graph which represents the mean radar height in terms of elapsed time. The soundings were performed with Darex J 11 balloons.

Table I

	time (min)	5	10	15	20	25	30	35	40	45	50	55	60
	mean balloon height (gpm)	1700	3300	4900	6600	8300	10100	11900	13800	15700	17600	19400	21300
$\lvert\Phi_r-\Phi_s\rvert$ (gpm)	0 - 100	14	10	11	10	10	8	7	2	3	3	-	-
	100 - 200	4	7	5	6	2	4	4	5	-	1	-	1
	200 - 500	-	1	2	1	5	5	5	9	8	3	5	4
	500 - 1000	-	-	-	1	1	-	1	1	5	5	4	4
	1000 - 2000	-	-	-	-	-	1	1	-	1	5	6	4
	2000 - 3000	-	-	-	-	-	-	-	1	1	-	2	3
	3000 - 4000	-	-	-	-	-	-	-	-	-	1	-	1
	4000 - 5000	-	-	-	-	-	-	-	-	-	-	-	-
	5000 - 6000	-	-	-	-	-	-	-	-	-	-	1	-
	> 6000	-	-	-	-	-	-	-	-	-	-	-	1
	maximum deviation in gpm. corresponding error in pressure (mb)	+180 18	+200 16	+220 14	+520 30	+860 41	+1130 45	+1670 51	+2170 50	+2920 50	+3880 49	+5060 50	+6160 50

We observe that there is a general trend for deviations to increase with height. Some deviations are enormous as can be seen in the last row where the observed maximum height differences are presented; it should be noted that these maximum figures refer to one particular radiosounding. It is pointed out that the number of positive deviations almost balanced the number of negative deviations. One could easily ask whether the great differences in simultaneous heights should not effect all aerological data in the TEMP report to such a degree that they are completely unfit for use in analysis.

To answer this question it is necessary to consider the effect in some more detail.

An error in the radar height is caused by errors in elevation angle and slant range. Since these are claimed to be less than 0.1° resp. 100 m, both systematically and random, it is impossible to

explain height differences of more than 200 m in the whole working area, say 100 km about the site of the station. As refraction normally plays a part only at very low elevation angles and the lowest observed elevation angle was above 10°, we state that the balloon height measured with the precision radar available during the experiments remained accurate within a few hundred meters.

An error in the sounding height depends on errors in the observed variables of state, p, T and U.

Consider equation (2) for Φ_s:

$$\Phi_s = - \int_{p_o}^{p} RT_v \, d\ln p$$

Then an error in Φ_s is given by

$$\delta\Phi_s = - \int_{p_o}^{p} R\delta T_v \, d\ln p - \int_{p_o}^{p} R \frac{\delta T_v}{\delta p} \delta p \, d\ln p - \frac{RT_v}{p} \delta p \Big|_{p_o}^{p} \ldots \qquad (3)$$

The first two terms on the right contribute to $\delta\Phi_s$ by a shift of the ascent curve (T, p) in the diagram. This shift is caused by errors both in T_v and p. The last term determines the effect caused by a change in the limits of integration.

When dealing with the geopotential of standard pressure surfaces the last term has to be left out of consideration as the limits of integration are fixed. However, when significant points like inversions, tropopause level, etc. are considered, the last term cannot be deleted and it can be shown that it is dominating the preceding two terms at least by a factor 10. It is this term which can explain the great differences between radar height and sounding height. Since only an increment δp is involved in this term, predominantly great errors in the pressure measurement are responsible for the observed height differences. A point S located on the (Φ_s, t) curve (cf. fig. 1), corresponding to a significant point in the temperature recording is displaced parallel to the

Φ-axis. However, as a deviation of 1 gpkm in a significant point corresponds with an error of a few gpdam in the geopotential of an adjacent standard pressure level, a point P on the (Φ_s, t) curve, corresponding to a standard pressure level, will shift <u>almost</u> parallel to the t-axis. This illustrates why the effect of the height difference is not clearly reflected in the data of temperature, humidity and geopotential of standard pressure levels.

The term causing the great deviations in height may be written:

$$\frac{RT_v}{p}\,\delta p = \delta p\ (\Delta\Phi)_{\delta p=1} \quad \cdots \qquad (4)$$

where $(\Delta\Phi)_{\delta p=1}$ denotes the change in geopotential corresponding to 1 mb change in pressure. In the last row of table I the figures in brackets represent the approximate errors in pressure δp, computed from (4) and table 57 of the Smiths. Tables. The large errors in pressure may be exceptional; they give rise to out-liers in the geopotential, sometimes observed in the upper air analyses.

3. <u>RASON diagram</u>

3.1. <u>General properties</u>

When observed pressure data are cancelled in computations of the aerological data and pressure is replaced by the radar height Φ_r it is necessary to design a new diagram in order to calculate all aerological data to be distributed to meteorological centra. The one described here has been given the name <u>Rason diagram</u> in order to indicate its use for simultaneous radar- and radiosonde observations without measurement of pressure. Part of a diagram is inserted in this report. Since the geopotential Φ plays an important part, the diagram is essentially a position or geopotential diagram, according to the classification in WMO publication: "Les diagrammes aerologiques" (WMO No. 66.TP.25).

As we consider a (Φ, T, U) method, the Cartesian coordinates should be functions of geopotential resp. temperature. The functional relationship depends on what we think to be the most important operation in the diagram. It will be obvious, that the

computation of pressure is the main goal to complete the set of values already known.

From the equation of state for moist air

$$p = \rho R T_v ,$$

the hydrostatic equation

$$dp = - g \rho \, dz$$

and the definition of geopotential

$$d\Phi = g \, dz ,$$

we derive

$$\frac{dp}{p} = - \frac{1}{R T_v} d\Phi \ \ldots \qquad (5)$$

Since T_v is known as function of Φ:

$$T_v = T_v(\Phi) ,$$

we find after integrating (5):

$$\ln p_2/p_1 = - \frac{1}{R} \int_{\Phi_1}^{\Phi_2} \frac{1}{T_v(\Phi)} d\Phi \qquad (6)$$

An alternate form of (6) is

$$\ln p_2 - \ln p_1 = - \frac{1}{R} \frac{\overline{T}}{T_v} (\Phi_2 - \Phi_1) \ \ldots \qquad (7)$$

where

$$\frac{\overline{T}}{T_v} = \frac{1}{T_v^*} = \frac{\int_{\Phi_1}^{\Phi_2} \frac{1}{T_v(\Phi)} d\Phi}{\int_{\Phi_1}^{\Phi_2} d\Phi} \ \ldots \qquad (8)$$

It follows from (6) and (7) that for pressure computations we must perform an integration of the reciprocal virtual temperature with respect to the geopotential. That is the reason why in the diagram $\frac{1}{T}$ and Φ are taken as abscissa and ordinate. Then the procedure to find $\frac{1}{T_v}$ is to evaluate $\frac{1}{T}$ first and apply a correction for humidity afterwards. This method is similar to that in thermo-dynamic diagrams, where the correction is determined by means of the virtual temperature increment for saturated air $(T_v - T)_s = T_{v,s} - T$ and relative humidity U. The temperature increment is usually shown there by scales along main isobars.

The abscissa in the diagram is also applied as a coordinate axis for the pressure in order to construct pressure-height curves, (p, Φ) curves. Besides, part of the temperature axis, that between -60° and -50°, is reserved for representing relative humidity in %. In the model inserted in this report the ICAO standard atmosphere is shown, mainly for the purpose of checking computations.

3.2. Use of the diagram

We examine a simultaneous observation with radar and a radiosonde. The radiosonde is equipped with temperature and humidity sensor elements only, or, when the pressure sensor element is not omitted, the pressure is left out of account.

The observed variables are recorded as function of time:

$$\begin{aligned} T &= T(t) \\ U &= U(t) \\ \Phi &= \Phi(t) \end{aligned} \qquad (9)$$

T and U are derived from transmitted radio signals in the usual manner. The geopotential Φ, the "radar height", is obtained from radar data as described in paragraph 2.

Since the parameter t in (9) should be eliminated it is essential that both radar and radiosonde observations are synchronized properly. In the Rason diagram corresponding values of Φ and T, resp. Φ and U are plotted. These values refer to significant points in the temperature record and to some inter-

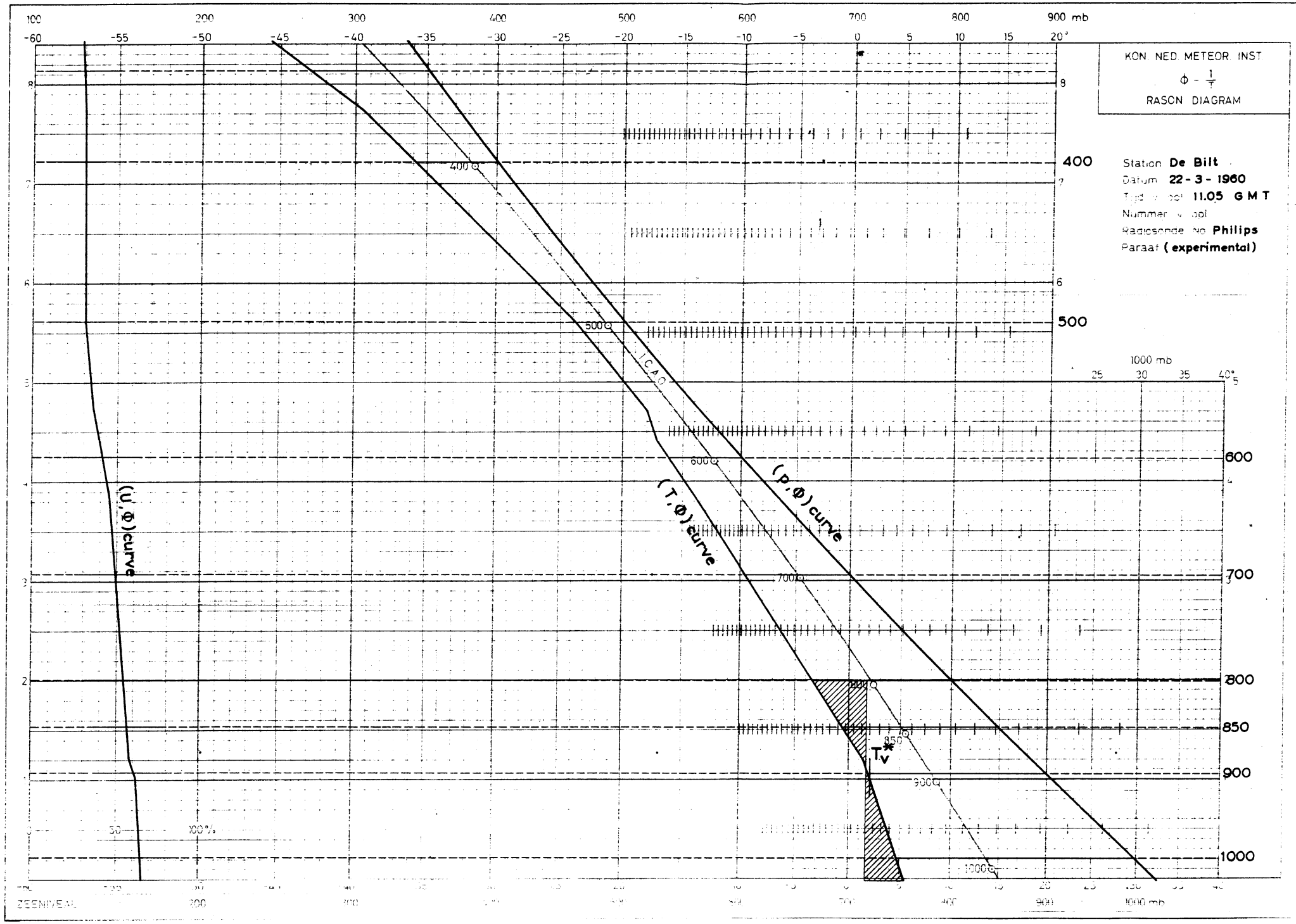
KON. NED. METEOR. INST
Φ - 1/T
RASON DIAGRAM
Station De Bilt
Datum 22-3-1960
Tijd v. opl. 11.05 G M T
Nummer v. opl.
Radiosonde No Philips
Paraaf (experimental)
100 200 300 400 500 600 700 800 900 mb
-60 -55 -50 -45 -40 -35 -30 -25 -20 -15 -10 -5 0 5 10 15 20°
1000 mb
25 30 35 40°
400
500
600
700
800
850
900
1000
400Θ
500Θ
600Θ
700Θ
800Θ
850Θ
900Θ
1000Θ
ICAO
(p,Φ) curve
(T,Φ) curve
(U,Φ) curve
T*v
50
100%
ZEENIVEAU

mediate points if necessary.

The computation of the data may proceed by different methods. One of them is presented here, because it has shown in practice to be competative in speed and accuracy with the conventional methods of computation in (p, T, U) soundings.

The method starts with a calculation of pressure and constructing a subsequent (p, Φ) curve.

Let Δp be the pressure increment in a layer between two levels having geopotential Φ_1 and Φ_2. Then we have

$$\Delta p = p_2 - p_1 = p_1\left(\frac{p_2}{p_1} - 1\right)$$

In view of (6), (7) and (8) Δp becomes

$$\Delta p = p_1 \left(\exp\left(-\int_{\Phi_1}^{\Phi_2} \frac{1}{RT_v}\, d\Phi\right) - 1\right)$$

$$= p_1 \left(\exp\left(-\frac{1}{RT_v^*}\,\Delta\Phi\right) - 1\right) \ldots \qquad (10)$$

where $\Delta\Phi = \Phi_2 - \Phi_1$.

For p = 1000 mb and $\Delta\Phi$ = 1 gpkm we obtain

$$\Delta^* p = 1000 \left(\exp\left(-\frac{1000}{RT_v^*}\right) - 1\right)$$

Then the pressure increment within a layer of 1 gpkm will be

$$\Delta p = \frac{p_1}{1000}\ \Delta^* p \ \ldots \qquad (11)$$

Values of the pressure increment $\Delta^* p$ between two levels having a geopotential difference of 1 gpkm and a pressure of 1000 mb in the lower level as a function of virtual temperature are to be found in table II.

Table II

°C	0	1	2	3	4	5	6	7	8	9
+30	106,5	106,2	105,9	105,5	105,2	104,9	104,6	104,2	103,9	103,6
+20	109,9	109,5	109,2	108,9	108,5	108,2	107,9	107,5	107,1	106,8
+10	113,5	113,2	112,8	112,4	112,0	111,7	111,3	110,9	110,6	110,2
+ 0	117,5	117,1	116,7	116,3	115,9	115,5	115,1	114,7	114,3	113,9
- 0	117,5	117,9	118,3	118,7	119,1	119,5	119,9	120,3	120,8	121,2
-10	121,7	122,1	122,6	123,0	123,4	123,8	124,3	124,8	125,3	125,7
-20	126,2	126,7	127,2	127,6	128,1	128,5	129,0	129,5	130,0	130,5
-30	131,0	131,5	132,0	132,5	133,0	133,5	134,1	134,6	135,2	135,7
-40	136,3	136,8	137,4	137,9	138,5	139,0	139,6	140,1	140,7	141,3
-50	141,8	142,4	143,0	143,7	144,3	144,9	145,5	146,1	146,8	147,4
-60	148,0	148,7	149,3	150,0	150,6	151,2	151,9	152,6	153,3	154,0
-70	154,7	155,4	156,1	156,8	157,5	158,3	159,0	159,7	160,5	161,2

Similar tables have been made for layers of 2, 3, 4 and more gpkm. The procedure to be applied for pressure computations may be summarized as follows:

a) Evaluate the pressure p_0 at mean sea level ($\Phi = 0$).

b) Determine the mean reciprocal virtual temperature $\frac{\overline{1}}{T_v} = \frac{1}{T_v^*}$ between mean sea level and the first "standard" level, i.e. 1 gpkm, 2 gpkm, etc. as well as each successive pair of standard levels.

c) Read $\Delta^* p$ from table II as a function of T_v^*.

d) Compute Δp from $\Delta^* p$, for the layer between mean sea level and the first standard level, inserting for p in equation (11) the pressure at mean sea level.

e) Compute $p = p_0 + \Delta p$.

f) Repeat the process for each successive pair of levels.

To determine the mean reciprocal virtual temperature $\frac{1}{T_v^*}$ a straight line is used to equalise areas in the $(\Phi, \frac{1}{T})$ ascent curve. The point of intersection of the straight line with the ascent curve fixes a value for $\frac{\overline{1}}{T}$.

$\frac{\overline{1}}{T}$ being known the mean reciprocal virtual temperature

$\frac{1}{T_v}$ is obtained, after a correction has been applied graphically for the humidity. To this aim the mean relative humidity U is read and multiplied with the reciprocal virtual temperature increment for saturated air $\left(\frac{1}{T} - \frac{1}{T_v}\right)_s$.

Indeed, we have

$$\left(\frac{1}{T} - \frac{1}{T_v}\right)_s = \frac{1}{T} - \frac{1}{T_{v,s}}$$

$$U\left(\frac{1}{T} - \frac{1}{T_{v,s}}\right) = \frac{U(T_{v,s} - T)}{T\,T_{v,s}}$$

$U(T_{v,s} - T)$ is the correction applied in most thermodynamic papers

$$U(T_{v,s} - T) = T_v - T$$

Therefore the correction becomes

$$\frac{U\,(T_{v,s} - T)}{T\,T_{v,s}} \approx \frac{T_v - T}{T\,T_v} = \frac{1}{T} - \frac{1}{T_v}$$

where T_v in the denominator has been substituted for $T_{v,s}$, a simplification that does not influence the result.

In the diagram the increment $\left(\frac{1}{T} - \frac{1}{T_v}\right)_s$ is read from scales which are shown on some main geopotential levels.

Through corresponding (p, Φ) points a curve is drawn. This is facilitated considerably by using a templet, the edge of which has been cut according to the (p, Φ) curve in the standard atmosphere.

As the tolerance in accuracy of the aerological data in significant points, the tropopause level and level of maximum wind is less stringent than that in standard pressure surfaces, the values such as temperature, geopotential and pressure are read directly from the (p, Φ), (T, Φ) and (U, Φ) graphs as usual.

In the standard pressure levels, however, a graphical determination of the geopotential Φ from the (p, Φ) graph, will be too rough. To obtain more accurate values an additional computation is made of the geopotentials using the "mean isotherm method" and applying the well-known Bjerknes tables. To this aim straight lines are drawn parallel with the T-axis, passing through the points of intersection of the (p, Φ) graph with the levels p = 1000, 900, 850 mb ... The points of intersection of the straight lines with the ascent curve determine the limits between which mean temperatures are to be found. In the Rason diagram the mean reciprocal virtual temperature should be established when entering the Bjerknes tables, for according to (7) and (8) we have

$$\ln p_2 - \ln p_1 = - \frac{1}{R T_v^*} (\Phi_2 - \Phi_1) ,$$

where

$$\frac{1}{T_v^*} = \overline{\frac{1}{T_v}} = \frac{\int_{\Phi_1}^{\Phi_2} \frac{1}{T_v} d\Phi}{\Phi_2 - \Phi_1}$$

Hence $\Phi_2 - \Phi_1 = - R T_v^* (\ln p_2 - \ln p_1)$.

On the other hand the (p, T, U) method gives

$$\Phi_2 - \Phi_1 = - R \overline{T}_v (\ln p_2 - \ln p_1) ,$$

where

$$\overline{T}_v = \frac{\int_{p_1}^{p_2} T_v d\ln p}{\ln p_2 - \ln p_1}$$

T_v is a mean value, obtained by preparing an integration graphically in thermodynamic diagrams like the Emagram ($\ln p$, T).

It follows that $T_v^* = \overline{T}_v$ or $\frac{1}{T_v^*} = \overline{\frac{1}{T_v}}$; in other words: the mean reciprocal virtual temperature in a Rason diagram corresponds to the reciprocal mean virtual temperature in an Emagram.

To calculate dew points T_d use can be made of different

kinds of graphical representations or tables, for instance the graph that indicates dew point difference as a function of relative humidity and temperature. If isopleths of saturation mixing ratio were printed on the diagram the dew point could be found by computing the actual mixing ratio that pertains to the dew point.

From the brief description above it may seem that the computation of aerological data in the (Φ, T, U) system is more time consuming than in the (p, T, U) system. This is correct, but the determination of the radar height is much easier than the determination of the pressure. That is the reason why the method in the Rason diagram has shown to compete in speed with a similar computation in the Stüve diagram.

The diagram could be completed with insertion of dry adiabats, saturated adiabats, isopleths of saturation mixing ratio and others. This would necessitate a reference to the standard atmosphere, as most of the quantities depend not on the geopotential but on pressure.

Dry adiabats form an exception, as we have

$$\frac{\delta T}{\delta \Phi} = 0.98 \ (^{\circ}C/100 \text{ gpm})$$

The dry adiabats therefore will practically run through the points of intersection of successive isotherms and geopotential levels.

4. Applications

4.1. Experiment with a Mark II B sonde and Philips sonde

On March 22, 1960, the present standard version of the Philips radiosonde was investigated by making an ascent together with a Kew Mark II B sonde. The balloon carrying the payload was a Darex J 11, tracked by the Decca windfinding radar. The simultaneous soundings were analysed both in Stüve and Rason diagrams.

The sondes were equipped with the following elements:

	Philips	Kew Mark II B
p	hypsometer	aneroïd
T	thermistor	bimetal
U	goldbeater's skin	goldbeater's skin

Figure 2 gives a graph of the sounding heights of both sondes and the radar height in terms of elapsed time after launching.

The sounding heights were obtained by computation of the geopotential of significant points and standard pressure levels. The radar height was derived from the radar data every minute.

As the anemometer cup wheel of the Mark II B sonde came to a stop at a point where the pressure was approximately 45 mb, the (Φ, t) curve of the British sonde terminates at point A (22250 gpm). The (Φ, t) curve of the Philips sonde terminates at point B, as the hypsometer circuit stopped oscillating.

The radar height is available up to the burst altitude and since the temperature and humidity circuits did function to the same altitude the sounding could be worked out in the Rason diagram up to the top of ascent (29200 gpm, 13,08 mb).

Part of the ascent of the Philips sonde is shown in the diagram.

It can be observed in fig. 2 that the sounding height of the Philips sonde practically coincides with the radar height even up to the end-point B. The sounding height of the British sonde, however, diverts considerably with respect to the radar height. The diversion begins between 300 and 200 mb and it increases up to the point where the recording of all elements stopped. The deviation there has become 1750 gpm. It is caused mainly by an error of more than 10 mb in the pressure (see table III).

In table III the figures in the left part denote pressure and temperature in <u>significant</u> points with respect to the temperature record of the Mark II B sonde. The right part gives values of p and T for corresponding points of the Philips sonde.

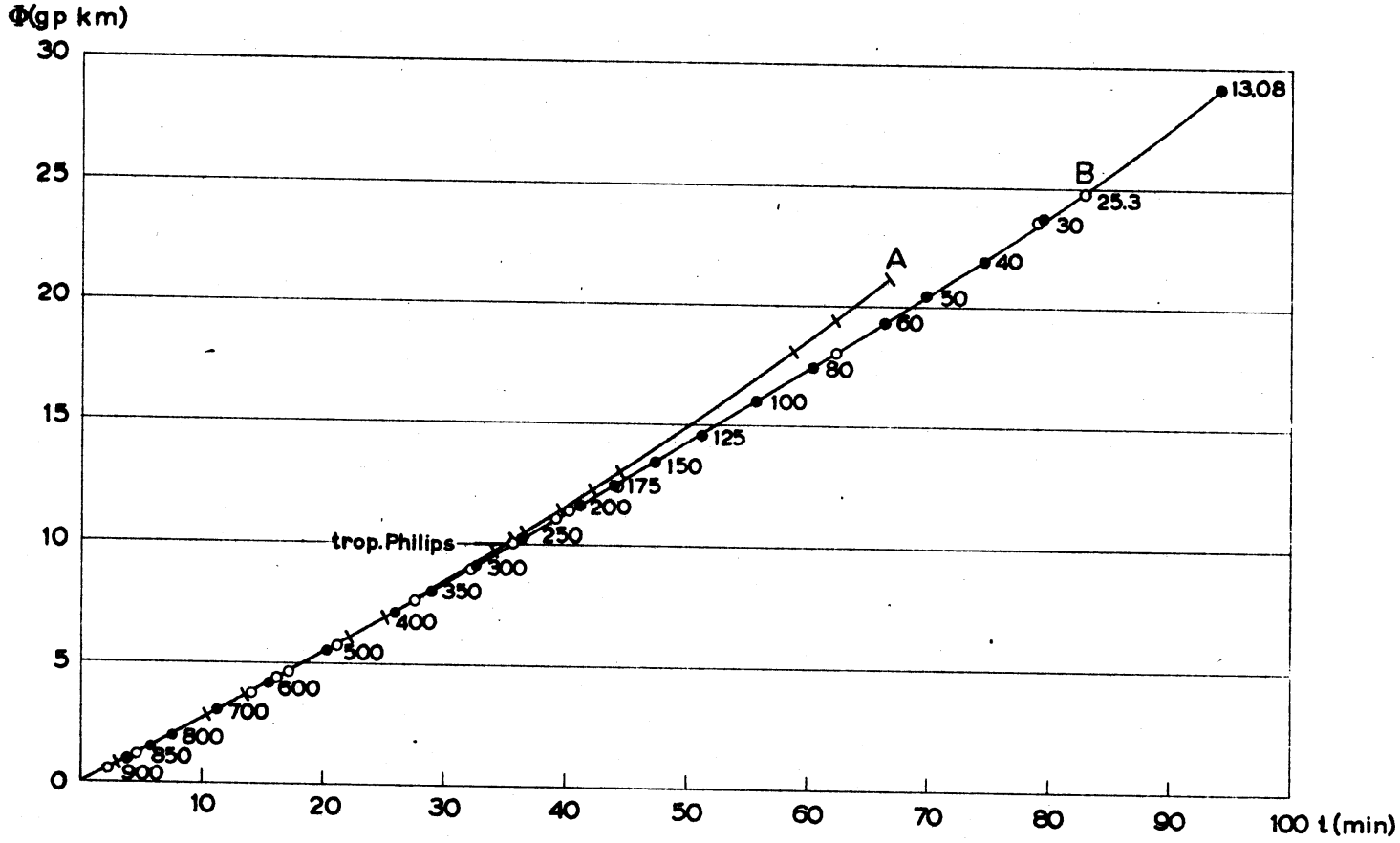
Φ(gp km)
30
25
20
15
10
5
0
13.08
B
25.3
30
40
50
60
80
100
125
150
175
200
250
300
350
400
500
600
700
800
850
900
A
trop. Philips
10
20
30
40
50
60
70
80
90
100 t (min)

Fig. 2

Table III

Mark II B		Philips			
p	T	p	T	Δp	ΔT
887	1.7	890	1.6	- 3	0.1
641	-13.6	645	-13.0	- 4	-0.6
492	-23.7	495	-24.1	- 3	+0.4
412	-32.3	414	-33.0	- 2	+0.7
268	-55.8	280	-55.5	-12	-0.3
trop. 250	-58.5	259	-57.9	- 9	-0.6
182	-58.5	193	-58.1	-11	-0.4
160	-54.2	171	-54.7	-11	+0.5
45	-54.4	58	-53.9	-13	-0.5

The last two columns represent the pressure, resp. temperature difference between the corresponding data. It can be seen that the temperatures agree within 0.7 °C. The pressure difference, a few mb at first, amounts to more than 10 mb in the higher levels. Undoubtedly the discrepancy in pressure accounts for the observed height difference. The significant point at 250 mb determines the tropopause level in the Mark II B ascent. In the Stüve diagram a geopotential of 10300 gpm is read from the (p,Φ) curve. The tropopause level in the Philips ascent amounted to 10080 gpm. Hence we can state that the error in the pressure element is responsible for a deviation in the tropopause level of more than 200 gpm. When examining the level of maximum wind a similar effect occurs.

In table IV geopotential and temperature are given of some standard pressure levels, which have been computed in the Stüve diagram as well as in the Rason diagram.

Table IV

	Philips				Kew Mark II B			
	Stüve		Rason		Stüve		Rason	
p (mb)	Φ (gpm)	T (°C)	Φ (gpm)	T (°C)	Φ (gpm)	T (°C)	p (gpm)	T (°C)
850	1525	- 0.5	1517	- 0.5	1522	- 0.4	1518	- 0.4
700	3050	- 9.7	3048	- 9.5	3049	- 9.2	3046	- 9.0
500	5579	-23.9	5575	-24.0	5579	-23.0	5575	-23.3
300	9115	-52.0	9107	-51.4	9130	-49.8	9110	-52.2
200	11683	-58.5	11672	-58.0	11695	-60.3	11673	-59.1
150	13516	-54.3	13505	-55.0	13518	-54.0	13504	-53.8
100	16120	-53.4	16111	-53.4	16124	-53.3	16111	-53
50	20587	-53.8	20582	-53.4	20596	-53.7	-	-
30	23860	-55.0	23852	-54.8	-	-	-	-
20	-	-	26453	-53.5	-	-	-	-
15	-	-	28304	-51.5	-	-	-	-

The table reveals that the values computed in the Rason diagram agree within a few meters, which can be explained by the small temperature differences of the thermistor in the Philips sonde and the bimetal in the British sonde. The difference between the Rason and Stüve data for the British sonde amounts to approximately 1 gpdam which probably is within accuracies, obtainable in the computation. Those between the Rason and Stüve data for the British sonde increase to approximately 2.5 gpdam in the tropopause region. Here the pressure error of the British sonde may account for the geopotential differences. It is noteworthy that only Rason data with respect to the Philips sonde are available up to burst altitude. Further it is observed that due to the pressure error of more than 10 mb in the Mark II B sonde, 50 mb data are given, but in reality the 50 mb level is not reached in the recording.

4.2. Re-evaluation of aerological data in 18 soundings

The aerological data originating from the set of 18 Mark II B

soundings have been recalculated in Rason diagrams.

The mean values of the geopotential differences in standard pressure levels as well as the maximum difference are presented in table V.

Table V

p	850	700	500	300	200	100	50
$\overline{\lvert \Phi_r - \Phi_s \rvert}$ (gpdam)	0.1	0.3	0.9	2.4	3.0	4.2	4.7
$\lvert \Phi_r - \Phi_s \rvert_{max}$ (gpdam)	1	1	2	11	8	17	7

Figures of this order of magnitude are not unfamiliar to a meteorologist. By mere inspection of the upper air charts it could be established that the "new" data were in better agreement with the analysis than the original data.

When comparing table I and table V we see once more, that the effect of large height deviations remains almost unobserved in the geopotential data in standard pressure levels of the TEMP report.

5. Discussion

It is well-known that the inconsistency of data in the upper air charts increases with height, so that analyses of say 50, 30 and 10 mb sometimes become illusive. This is the case when for instance light stratosferic winds prevail and accordingly the variance of the geopotential is small. Then the "noise factor", being the ratio between the instrumental error and the variance may increase to such high values, that the errors obscure the patterns of the state variables.

The accuracy required in the pressure observation amounts to something like 0.1 mb. To explain this, we should remind that a change in pressure of 1 mb at, say 30 km in the standard atmosphere corresponds to a change in height of 550 m. Such a high measure of

precision (0.1 mb) is at present unattainable. Therefore, the (Φ, T, U) method promises to be the best one to replace the (p, T, U) method.

Not only in the higher levels of the atmosphere this method is attractive, but also in the lower layers and the investigation of the 18 soundings has shown that in standard pressure levels like 500, 300, 200 mb and tropopause level the Rason data are much better than the Stüve data.

Further research must be undertaken to see the effect on the homogeneity of aerological networks. For instance by recalculating the aerological data in the (Φ, $\frac{1}{T}$) diagram at stations where in addition to the radiosonde observation winds are measured with a precision radar.

With an electrical temperature and humidity transducer like a thermistor and lithium chloride cell the (Φ, T, U) system is all-electric.

In principle the system may also be performed, after the burst altitude is reached and the sonde returns with a parachute. Especially when a sonde with humidity and temperature element is ejected from a rocket this method gives good prospects.

A further simplification would be to replace the radar height by the height determined from the ascent rate of the balloon or by a mean ascent curve. This has been investigated in the set of 18 Mark II B soundings. A mean ascent curve was computed and with the (Φ, t) curve the aerological data were again calculated in the Rason diagram. The new mean geopotential difference of standard pressure levels appeared to be almost equal to those in table V (sic), but the dispersion of the individual ascent curves was still too large to introduce a standard (Φ, t) curve.

The (Φ, T, U) method yields profits not only with respect to the accuracy of aerological elements but also financially. In addition, the frequency range, reserved for the pressure element, can be assigned to special instruments which have been constructed for physical research.

When a new radiosonde comparison would be undertaken by WMO the (Φ, T, U) method would be of utmost importance to combine the programme of radiosonde measurements with exact and synchronous measurements of the radar height.